Microstructure of *N*-Isopropylacrylamide−Acrylic Acid Copolymer Gels Having Different Spatial Configurations of Weakly Charged Groups

Fumiyoshi Ikkai,*,† Takuya Suzuki,‡ Takeshi Karino,‡ and Mitsuhiro Shibayama‡

L'Oreal Recherche, Nihon L'Oreal K.K., KSP R&D-D637, 3-2-1 Sakado, Takatsu-ku, Kawasaki, Kanagawa 213-0012, Japan, and The Institute for Solid State Physics, The University of Tokyo, 5-1-5 Kashiwanoha, Kashiwa, Chiba 277-8581, Japan

Received September 25, 2006; Revised Manuscript Received December 20, 2006

ABSTRACT: Gel microstructure formation according to spatial configuration of charged groups in gel network has been investigated using macroscopic swelling measurements and microscopic small-angle neutron scattering. Three types of gel consisting of hydrophobic *N*-isopropylacrylamide (NIPAm) and weakly charged acrylic acid (AAc) copolymers were prepared with different distributions of AAc monomer units in the network. The first type was a NIPAm/AAc copolymer gel in which NIPAm and AAc were randomly copolymerized in monomer units using the redox method. The second type was a UV-cross-linked NIPAm/poly-AAc copolymer gel in which NIPAm was copolymerized with polymer units of AAc. The third type was a NIPAm/poly-AAc polymer gel prepared using the redox method in which poly-AAc was not cross-linked but physically entrapped in the NIPAm polymer network. These three types of gel contained the same amount of charged groups but with different spatial configurations. The differences in spatial and topological distribution of charged groups were reflected in different responses regarding swelling properties and different microscopic structure upon temperature variation that we discussed with the concept of counterion condensation.

Introduction

Gels of *N*-isopropylacrylamide (NIPAm: CH_2═CHCONHCH-$(CH_3)_2$) copolymers with charged monomer, e.g., acrylic acid (AAc: CH_2═CHCOOH), have been a focus of constant attention as one of environment-responsive materials. One of the archetypal phenomena is known as "microphase separation"[1−7] in a poor solvent and the related characteristic "volume phase transition",[8−18] i.e., a discrete gel-volume shrinking. In the case of NIPAm/AAc copolymer gels, since NIPAm is a temperature-sensitive polymer, the microphase separation of NIPAm/AAc gel and the following volume phase transition occur at a critical temperature, T_{VPT}, depending on the surrounding temperature. T_{VPT} is around 34 °C for NIPAm homopolymer gels, and it rises with increasing charged AAc units. Microphase separation in a NIPAm/AAc copolymer gel has been interpreted as coexisting states of a swollen phase (ionized hydrophilic parts, i.e., AAc-rich domain) and a shrunken phase (hydrophobic parts, i.e., NIPAm-rich domain) at the microscopic level. Indeed, small-angle neutron scattering (SANS) studies revealed that the long period of microphase separation was hundreds of angstroms.[1,2,6,19−22] Many theoretical works predicted that the long period of microphase separation depended on various factors such as Flory's interaction χ parameter, the degree of ionization, salt concentration, and cross-linking density.[23−27] In previous decades, Tanaka et al.[28−30] asserted that such microphase separation and volume phase transition behavior were strongly related to life activities in biological body, and these phase changes are caused by competition between inter/intramolecular interactions such as electrostatic, hydrophobic, van der Waals forces, and hydrogen bonding. Indeed, Annaka and Tanaka found out a multiple volume phase transition, in which a gel could maintain different stable phases depending on its transition pathway.[29] They concluded that this multiple-phase behavior resulted from intermolecular interactions competing in a gel network. In other words, it means that alterations of "chain conformation" in a gel network can draw this unique multiphase separation of polymer gels.

However, alterations of "chain configuration" in gel-making process could be far more decisive for gel structure than alterations of "chain conformation". That is, random/nonrandom configuration of polymers could play a prominent role in determining gel microstructures. Now, we pay attention to spatial configuration of charged groups in weakly charged polymer gels. As far as we know, most of the theories on gels assume that charged groups are randomly distributed in the polymer network as "monomer units". Indeed, the degree of ionization, one of the most determining factors in the gel structure, has been considered as an average level in the overall gel. Furthermore, since radical polymerization was mostly used in gel preparation, hydrophobic and hydrophilic monomers were randomly copolymerized into gel network. In such a case, alteration of "chain conformation" in gel network may only arise from changes in preparation conditions. We recently developed a polymerization method that allows one to prepare a gel without using cross-linker. Owing to high photon energy of ultraviolet (UV) light involved, cross-linking reaction and polymerization take place simultaneously. Using this method, we successfully prepared different types of NIPAm/AAc copolymer gel in which AAc was distributed either as monomer or as polymer units.[31] It was achieved through UV-induced copolymerization of poly-AAc in an aqueous solution. Thus, NIPAm/AAc copolymer gels with different types of "chain configurations" could be investigated. The present study aimed to identify structural determining effects when altering network conformation and configuration in a weakly charged copolymer gel system consisting of NIPAm and AAc units, i.e., how spatial configuration of charged

* Corresponding author: Tel +81-44-812-2013; Fax +81-44-812-2033; e-mail fikkai@rd.loreal.com.
† Nihon L'Oreal K.K.
‡ The University of Tokyo.

10.1021/ma062216c CCC: $37.00
Published on Web 01/26/2007

groups affected gel microstructure formation and the inhomogeneities.

Theoretical Background

Swelling Behavior. For neutral polymer gels, a swelling equilibrium is achieved when the gel osmotic pressure, Π, becomes zero. Here, Π involves two contributions, i.e., the mixing effect of network polymer with solvent, Π_{mix}, and gel elastic effect, Π_{ela}, as expressed by the following Flory−Rehner type equation:[32,33]

$$\Pi = \Pi_{mix} + \Pi_{ela} \tag{1}$$

$$\Pi_{mix} = -(k_B T/V_s)[\ln(1-\phi) + \phi + \chi\phi^2] \tag{2}$$

$$\Pi_{ela} = \nu k_B T[(1/2)(\phi/\phi_0) - (\phi/\phi_0)^{1/3}] \tag{3}$$

where k_B, T, V_s, and υ denote the Boltzmann constant, the absolute temperature, the molar volume of the solvent, and the number of effective polymer chains per unit, respectively. ϕ and ϕ_0 are the polymer volume fractions at swelling equilibrium and at sample preparation time, respectively. χ is the Flory−Huggins interaction parameter. It is known that χ depends on T and ϕ, as given by

$$\chi = \chi_1 + \chi_2\phi \tag{4}$$

where

$$\chi_1 = (\Delta H - T\Delta S)/k_B T \tag{5}$$

and χ_2 is a constant. ΔH and ΔS are the enthalpy and entropy of mixing per monomeric unit, respectively. According to Hirotsu's work on NIPAm homopolymer gels, the following values are estimated, i.e., $\chi_2 = 0.518$, $\Delta H = -12.46 \times 10^{-21}$ J, and $\Delta S = -4.717 \times 10^{-23}$ J/K.[34]

The ν value is stoichiometrically estimated for NIPAm gels as follows:

$$\nu = \frac{2C_{cl}}{C_0}\frac{\phi_0}{V_p} \tag{6}$$

where C_{cl}, C_0, and V_p denote the cross-linker concentration, the initial monomer concentration, and the molar volume of monomeric unit, respectively. However, in the case of gelation process of concentrated monomer solutions, the prepared gel network is likely to have a large number of entanglements, which act as additional cross-linkers. Shibayama et al. assumed that the effect of the additional cross-linker was proportional to C_0 and proposed the modified Flory−Rehner equation, in which ν is altered to ν_e as follows:[32]

$$\nu_e \equiv \nu(\phi_0/\phi_{0,ref}) = \nu(C_0/C_{0,ref}) \tag{7}$$

where $\phi_{0,ref}$ and $C_{0,ref}$ are the lowest monomer volume fraction and concentration, respectively, when a uniform gel could be formed without the additional cross-links due to polymer entanglements.

Consequently, the condition of swelling equilibrium is expressed by the following equation:

$$\nu\frac{C_0}{C_{0,ref}}\left[\frac{1}{2}\left(\frac{\phi}{\phi_0}\right) - \left(\frac{\phi}{\phi_0}\right)^{1/3}\right] = \frac{1}{V_s}[\ln(1-\phi) + \phi + \chi\phi^2] \tag{8}$$

RP Theory for SANS. Microphase separation of weakly charged gels is described with Rabin−Panyukov theory (RP theory).[26] The RP theory properly describes the frozen inhomogeneities in addition to two opposite interactions, i.e., electrostatic (repulsive) and hydrophobic (attractive), on the basis of a mean-field theory of polymer gels. The theoretical structural factor, $S(q)$, consists of two contributions: one from static inhomogeneities, $C(q)$, and the other one from thermal concentration fluctuations, $G(q)$, where q is the scattering vector. Both $C(q)$ and $G(q)$ are built up with well-defined parameters, i.e., the average degree of polymerization between cross-links, N, the polymer volume fraction (polymer concentration), ϕ, the degree of ionization, f, and temperature, T (or the Flory's interaction parameter, χ). Here, we define N as $N = [(C_0 + 2C_{cl})/2C_{cl}]$. Using two sets of parameters, i.e., those at sample preparation time, ϕ_0, f_0, χ_0, in addition to those at observation time ϕ, f, χ, $S(q)$ is given by eqs 9, 10, and 11:

$$S(q) = G(q) + C(q) \tag{9}$$

$$G(q) = \frac{\phi N g(q)}{1 + w(q)\, g(q)} \tag{10}$$

$$C(q) = \frac{\phi N}{[1 + w(q)\, g(q)]^2(1+Q^2)^2}\left[6 + \frac{9}{w_0(q) - 1 + (1/2)Q^2(\phi_0/\phi)^{2/3}\phi_0^{-1/4}}\right] \tag{11}$$

where the subscript 0 means the parameter value at sample preparation time. a and $w(q)$ denote the segment length (8.12 Å for NIPAm polymer chains[1,35]) and the effective second virial coefficient, respectively. Q ($= aN^{1/2}q$) is the dimensionless wave vector. The function $g(q)$ is given by eq 12:

$$g(q) = \frac{1}{Q^2/2 + (4Q^2)^{-1} + 1} + \frac{2(\phi/\phi_0)^{2/3}\phi_0^{1/4}}{(1+Q^2)^2} \tag{12}$$

The functions of $w(q)$ and $w_0(q)$ are expressed by eqs 13 and 14, respectively:

$$w(q) = (1 - 2\chi + \phi)\phi N + \frac{l_B f^2 \phi N^2}{Q^2 + l_B f \phi N} \tag{13}$$

$$w_0(q) = \phi_0^{5/4}N + \frac{l_B f_0^2 \phi_0^{5/4} N^2}{Q^2(\phi_0/\phi)^{2/3} + l_B f_0 \phi_0^{5/4} N} \tag{14}$$

l_B is the dimensionless Bjerrum length given by $l_B = 4\pi L_B/a$, where L_B is the Bjerrum length set at 7 Å for aqueous solutions at 25 °C.

Experimental Section

Samples. *N*-Isopropylacrylamide (NIPAm), acrylic acid (AAc) *N*,*N*′-methylenebis(acrylamide) (BIS), ammonium persulfate (APS), and *N*,*N*,*N*′,*N*′-tetramethylethylenediamine (TEMED) were purchased from Wako Chemical Co. Ltd., Tokyo. NIPAm and AAc were purified before use by recrystallization and distillation, respectively. On the other hand, poly-AAc (M_w = 118 000) was purchased from Polymer Science Co. Ltd. and used without further purification.

Gel Preparation. Three types of NIPAm/AAc copolymer gel were prepared using two polymerization methods. Figure 1 shows diagram models of the structure of these copolymer gels. The lattice-shaped boxes represent gel networks, where thin lines and bold dots along the grids correspond to NIPAm chains and AAc monomer units, respectively. The first type is NIPAm/AAc

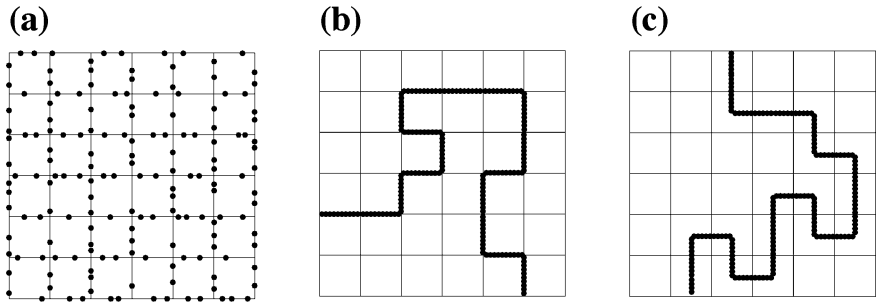

Figure 1. Diagram models of NIPAm/AAc gel networks: In (a) and (b), AAc components (thick parts) were copolymerized in monomer and polymer units, respectively. In (c), the AAc polymers were interpenetrated in gel network but not cross-linked. It should be noted that average charge density in each network is the same.

copolymer gel in which NIPAm and AAc are randomly copolymerized in monomer units using conventional redox polymerization (code: redox-mono-AAc) (Figure 1a).[1,20] The second type is NIPAm/poly-AAc copolymer gel in which poly-AAc is copolymerized with NIPAm by UV-induced polymerization method (code: UV-poly-AAc) (Figure 1b).[31,36] The third type is a NIPAm/poly-AAc polymer gel prepared from NIPAm and poly-AAc using the redox polymerization method and in which AAc polymers are physically entrapped in a NIPAm network but not cross-linked (code: redox-poly-AAc) (Figure 1c). It should be noted that these three types of gel have the same degree of ionization, i.e., the same ratio of AAc units to NIPAm, but different spatial configurations of charged groups.

Gels corresponding to Figure 1a−c were prepared as follows. For redox-mono-AAc gel, 668 mM NIPAm and 32 mM AAc were dissolved in 10 mL of water. Then, 7 mM BIS and 1.54 mM APS were added to the solution as cross-linker and redox initiator, respectively. After further addition of 24 μL of TEMED as accelerator, the solution was kept at 20 °C for 24 h to achieve gelation. For UV-poly-AAc gel, an aqueous solution containing 668 mM NIPAm, 32 mM (calculated as monomer units) poly-AAc (M_w = 118 000), and 20 mM APS (as UV photoinitiator) was gelled by UV irradiation for 1 h at 20 °C. UV irradiation was performed using a 500 W Deep-UV lamp (USHIO Inc., Tokyo, Japan) with an illuminance spectrum at $\lambda \leq 300$. In the case of UV-cross-linked gelation, radicals generated by UV irradiation attack acryloyl-type monomers and polymers, resulting in direct cross-linkings between them without any cross-linkers as well as some degradation.[31,36] In UV-induced NIPAm/poly-AAc gelation, poly-AAc was therefore chemically cross-linked to the NIPAm network. For redox-poly-AAc gel, 668 mM NIPAm, 32 mM (calculated as monomer units) poly-AAc, 7 mM BIS, 1.54 mM APS, and 24 μL of TEMED were dissolved in 10 mL of water and then gelled at 20 °C for 24 h. Here, poly-AAc is contained in the gel network but is not cross-linked to the network because of the absence of cross-linker and reactive groups on poly-AAc chains. Redox-reacted and UV-cross-linked gels were prepared in 8 mm diameter Pyrex test and quartz-test tubes, respectively, in a water-circulating thermobath. For SANS measurements, all gels prepared were taken out of the test tubes and smashed through a 500 μm sieve. Then, gels were washed with a large amount of water for 3 days under stirring. It should be noted that, for redox-poly-AAc, extraction of a small amount of unconnected poly-AAc might occur during washing. However, in a series of dynamic light scattering (DLS) experiments for unwashed reactor-batch redox-poly-AAc, agreement of volume phase transition temperature between the swelling measurements and the DLS was observed.[37] This fact suggests that poly-AAc was strongly trapped even after washing. After freeze-drying, a given amount of deuterium water (D_2O) was added to be ϕ (the gel volume fraction) = 0.1. For swelling measurements, all gel samples were prepared in a narrow quartz capillary (800 μm diameter) with the same recipes as those for SANS. The details of swelling measurements are described elsewhere.[15]

SANS. Small-angle neutron scattering (SANS) experiments were carried out using a two-dimensional SANS spectrometer (SANS-U) of Institute for Solid State Physics, University of Tokyo, located at JRR3M in Japan Atomic Energy Agency (JAEA), Tokai, Japan.[38] The SANS intensity functions were collected at room temperature for 1.5 and 8 h at a 2 and 8 m sample-to-detector distance, respectively. 1 wt % gel samples in quartz cells with 4 mm optical path were irradiated with a 7.0 Å wavelength neutron beam. The wavelength distribution of the incident neutron beam, $W_\lambda(\lambda)$, is known to be $W_\lambda(\lambda) = 0.1$. The scattered intensity was circularly averaged and rescaled to the absolute intensity scale with a polyethylene secondary standard calibrated for the incoherent scattering from vanadium.[39] The solvent correction for scattered intensity was made using eq 15:

$$I(q) = I_{\text{sample}}(q) - (1 - \phi_p) I_{D_2O}(q) - I_{\text{incoh}}(q) \qquad (15)$$

where $I_k(q)$ denotes the observed scattering intensity in absolute scale of the kind k (= gel sample, D_2O, and the incoherent scattering of the NIPAm monomer solution) and ϕ_p is the volume fraction of the polymer.

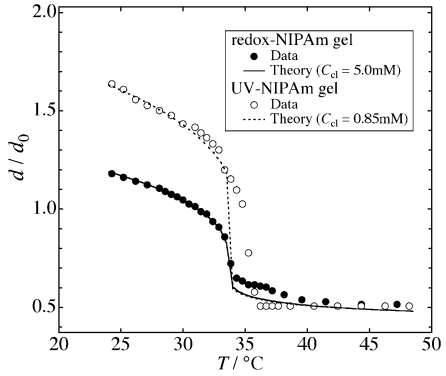

Figure 2. T dependence of swelling behavior of redox-polymerized NIPAm (closed circles) and UV-cross-linked NIPAm (open circles) gels.

Results and Discussion

Estimation of Effective Cross-Linker Concentration. When we discuss swelling behavior of polymer gels, the number of cross-links of gel is one of the most important parameters to determine the swelling degree. Since two kinds of gelation methods were used in this study, we first estimated the difference of cross-linking capability of these methods. Figure 2 shows the temperature, T, dependence of swelling behaviors of redox-polymerized NIPAm (redox-NIPAm; closed circles) and UV-cross-linked NIPAm (UV−NIPAm; open circles) gels. The diameter, d, was normalized with an inside diameter of capillary, d_0, in which the gels were prepared. It should be noted that $d/d_0 = (\phi_0/\phi)^{1/3}$. Each swelling behavior was fitted with eq 8, as shown by solid curves in the figure. It is well-known that redox-NIPAm gel has a volume phase transition temperature, T_{VPT}, near 34 °C, at which the gel shrinks dramatically. This is due to hydrophobic property of NIPAm polymer. Unexpectedly,

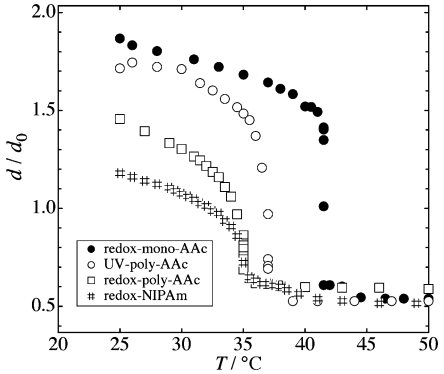

Figure 3. *T* dependence of swelling behavior of three types of NIPAm/AAc gel: # is for NIPAm homopolymer gels. The T_{VPT} is ca. 35 °C for redox-NIPAm and redox-poly-AAc gels, ca. 37 °C for UV-poly-AAc gels, and ca. 42 °C for redox-mono-AAc gels.

however, it was observed that both T_{VPT} and the swelling degree depended on the gelation method. Though T_{VPT} generally depends only on the degree of ionization in gel network, the reason for the shift of T_{VPT} difference is not clear. One possible reason is that residual APS is chemically bonded to NIPAm chains (and/or it induces hydrolysis of NIPAm chains). The amount of APS used in UV-cross-linked gelation was more than 10 times larger than that in redox-polymerized gelation. Thus, a far larger amount of APS ends may remain after UV-induced gelation than after redox gelation and act as charged groups in the network polymer. Here, we assume that T_{VPT} of UV-NIPAm gel is the same as that of redox-NIPAm gel.

Using eq 8, we evaluated effective cross-linker concentration for both types of gels. In eq 8, $C_{0,ref}$, V_p, and V_s for NIPAm/water gel system are 200 mM (as evaluated in the previous paper),[32] 103 cm^3/mol, and 18 cm^3/mol, respectively. The effective cross-linker concentration was estimated to be 5 mM for redox-NIPAm gel and 0.85 mM for UV−NIPAm gel. It should be noted that the feed for redox-NIPAm gel was 0.02 (C_{BIS} = 7 mM) for both types of gel. In the following discussion, we therefore use thus evaluated values of C_{cl}, i.e., 5 mM for redox-mono-AAc and redox-poly-AAc gels and 0.85 mM for UV-poly-AAc gel.

Swelling Behavior. Figure 3 shows *T* dependence of swelling behavior for the three types of gel, with the swelling curve of redox-NIPAm as a reference. In general, NIPAm gels containing AAc as copolymerized component have a higher T_{VPT} and a larger swelling degree than NIPAm homopolymer gels. This is interpreted as resulting from hydrophilic effect of AAc units. It should be noted that, although the three types of NIPAm/AAc gel, i.e., redox-mono-AAc, UV-poly-AAc, and redox-poly-AAc gels, have the same amount of AAc units, large differences in swelling behavior and T_{VPT} are found. The redox-mono-AAc gel (closed circles) had the highest T_{VPT} (≈42 °C) and swelling degree below T_{VPT} ($d/d_0 \approx 1.9$ at 25 °C). The UV-poly-AAc gel (open circles) comes after with $T_{VPT} \approx 37$ °C, and $d/d_0 \approx 1.8$ at 25 °C. On the other hand, redox-poly-AAc gel (open squares) showed the lowest T_{VPT} (≈35 °C), which is similar to redox-NIPAm gel (sharp), though the swelling degree below T_{VPT} ($d/d_0 \approx 1.4$ at 25 °C) is somewhat higher than that of redox-NIPAm gel. It should be noted here that the difference between chemically entrapped (UV-poly-AAc) and physically entrapped (redox-poly-AAc) gels is clear. It is known that the pK_a = 5.6 for poly-AAc. Hence, a full ionization is attained at pH 9. As a matter of fact, we reported pH dependence of the swelling ratio for the PNIPAm/AAc gel, and full ionization was attained at pH 7 and above.[3]

SANS. Figure 4 shows the *T* dependence of SANS profiles, $I(q)$, of each type of NIPAm/AAc (668 mM/32 mM) copolymer gel. Parts a, b, and c of Figure 4 show the SANS results of the gels corresponding to parts a, b, and c of Figure 1, respectively. Here, the solid lines in the graphs denote theoretical fitting curves described below. The $I(q)$s in the figures can be categorized according to three types of scattering function: category I: S-shaped decreasing functions without scattering peak observed exclusively below T_{VPT}; category II: one-peaked functions observed above T_{VPT}; category III: power law functions with a slope close to −4 observed above T_{VPT}.

Structures below T_{VPT}. In Figure 4a, $I(q)$s for $T < T_{VPT}$ (≈42 °C) were fairly simple decreasing functions, except for small rising at the lower *q* region. They were well fitted with a modified squared Lorentz (SL) function:[2,40]

$$I(q) = \frac{I_L(0)}{1 + \xi^2 q^2} + \frac{I_{SL}(0)}{(1 + \xi^2 q^2)^2} + I_e(0) q^{-3.6} \qquad (16)$$

Here, the second term of the right-hand side of eq 16 is based on the so-called Debye−Bueche function,[41,42] and ξ denotes a correlation length of concentration fluctuations in gel network. $I_L(0)$ and $I_{SL}(0)$ are the zero-*q* intensities corresponding to the dynamic and static contributions to $I(q)$. It should be noted that the adoption of one correlation length in eq 16 is based on statistical theory on polymer gels, in which the correlation length corresponds to the Edwards screening length, i.e., the excluded-volume effect.[43] With this correlation length by introducing a coupling constant, a correlation length related to static inhomogeneities should be described.[40] The last term, $I_e(0)q^{-3.6}$, introduced by Horkay et al.[44] describes the upturn at the low-*q* region. This term is rather controversial, and its physical implication has not been clarified yet. In Figure 4b, $I(q)$s for $T < T_{VPT}$ (≈37 °C) are also decreasing functions, but the shapes of the functions are very different from those of redox-mono-AAc gel at $T < T_{VPT}$. In particular, $I(q)$s of redox-poly-AAc gel (Figure 4b) are convex-upward functions with respect to *q* at $q \leq 0.03$ Å^{-1}. Such functions no longer fitted with the SL plot but rather the phenomenological Gauss−Lorentz (GL) plot,[45−48] which is given by

$$I(q) = \frac{I_L(0)}{1 + \xi^2 q^2} + I_G(0) \exp\left(-\frac{R_g^2 q^2}{3}\right) \qquad (17)$$

where the existence of randomly distributed static inhomogeneities with a characteristic mean size of R_g is assumed, as shown by the second term of the right-hand side of eq 17.

In Figure 4c, $I(q)$s for $T < T_{VPT}$ (≈33 °C) can also fit with eq 16. For all gels at $T < T_{VPT}$, ξ increases with *T* as shown in Figure 5. This ξ behavior seems to be reasonable because the concentration fluctuations become large when approaching T_{VPT}.[45] Note that ξ for redox-mono-AAc gel is the smallest and that for UV-poly-AAc gel the largest of the three types of gel. In redox-mono-AAc gel, weakly charged groups were dispersed in monomer units, so the period of concentration fluctuations is inherently small. In UV-poly-AAc gel, on the other hand, the existence of large-scale inhomogeneities, which was proved by R_g component in Figure 4b, affects the concentration fluctuations. Here, R_g (shown with the right axis) changed from ca. 120 to 135 Å, which may correspond to that of a random coil with excluded volume for a poly-AAc chain. Unlike weakly charged groups in redox-mono-AAc gel, poly-AAc's in UV-poly-AAc gel are localized in polymer units, leading to larger concentration fluctuations.

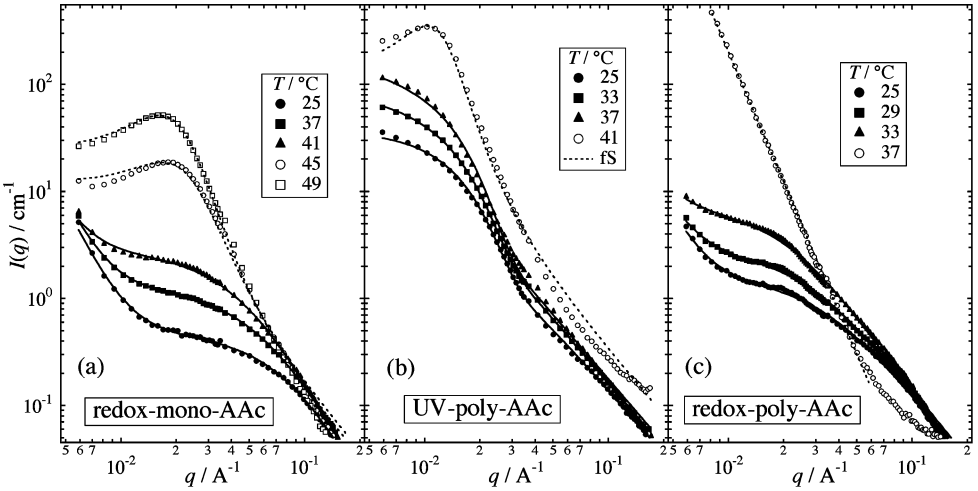

Figure 4. *T* dependence of SANS profiles, *I*(*q*), for each type of gel network consisting of NIPAm and AAc. Solid lines show theoretical fitting curves.

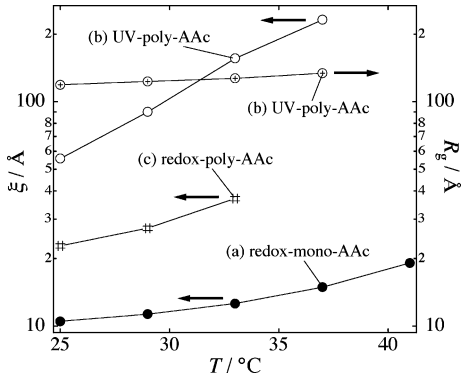

Figure 5. *T* dependence of ξ and R_g for three types of NIPAm/AAc gels.

Table 1. Comparison of SANS Fitting Parameters between Redox-mono-AAc (at 49 °C) and UV-poly-AAc Gels (at 41 °C)

	T (°C)	*N* (C_{cl}/mM)	f (=f_0)	ϕ (=ϕ_0)	χ
redox-mono-AAc	49	71 (5)	0.0457	0.1	0.79
UV-poly-AAc	41	417 (0.85)	0.0184	0.1	0.64

Structures above T_{VPT}. As shown in Figure 4a,b, a broad peak appears in *I*(*q*)s at $q = 0.01-0.02$ Å^{-1} for redox-mono-AAc and redox-poly-AAc gels above T_{VPT} (≥45 °C), which cannot be described by the SL equation (i.e., eq 16). For a theoretical fitting with this broad peak, we employed Rabin−Panyukov (RP) theory,[26,49] assuming that the peak originated from weakly charge-induced microphase separation in a poor solvent. RP fittings were quite successful for *I*(*q*) at 49 °C (Figure 4a) and for *I*(*q*) at 41 °C (Figure 4b). Table 1 shows the fitting results. The *I*(*q*) at 49 °C for redox-mono-AAc gel fitted with $N = 71$, ϕ (=ϕ_0) = 0.1, f (=f_0) = 0.0457, and χ = 0.79. On the other hand, the *I*(*q*) at 41 °C for UV-poly-AAc gel was reproduced with $N = 417$, ϕ (=ϕ_0) = 0.1, f (=f_0) = 0.0184, and $\chi = 0.64$. Since *N* and ϕ (=ϕ_0) are fixed according to the gel preparation condition, the peak position difference depends on f and χ. The f value of 0.0457 for redox-mono-AAc gel corresponds to the feed ratio of AAc, i.e., 32/(668 + 32). Full ionization of AAc in a gel can be assumed since AAc concentration is low. However, the evaluated value of ϕ was 0.0184 for UV-poly-AAc gel. This is much lower than the feed ratio of AAc.

It is important to understand how the structural parameters, including f and χ, affect gel microstructure in RP theory. Figure 6 shows the simulated structure factor, *S*(*q*)s, with respect to (a) f (=f_0), (b) ϕ, (c) χ, (d) c_s (the salt concentration), and (e) *N*. The parameters fixed in each figure were chosen according to those of our fitting results, i.e., f (=f_0) = 0.0457, ϕ (=ϕ_0) = 0.1, $\chi = 0.79$, $c_s = 0$, and $N = 50$. The thick *S*(*q*) function curve in each figure is the reference curve obtained with the "fitted" parameters. *S*(*q*) has a peak around $q = 0.01-0.02$ Å^{-1}, corresponding to a long period of the microphase separation (=$2\pi/q$). The thick dotted lines in (a)−(e) shows trajectories of peak position during a scan of one of the parameters, such as f for (a), ϕ for (b), χ for (c), c_s for (d), and *N* for (e). Two important features can be drawn from this simulation. One is that the peak of *S*(*q*) becomes sharper with decreasing f or increasing ϕ, χ, c_s, and *N*, indicating that the gel is in a poor solvent. Then, by crossing a critical value of the parameter, a macroscopic phase separation occurs. Another feature is that the peak position, q_{peak}, shifted to a smaller q with increasing f for (a) or c_s for (d) or decreasing ϕ for (b) or χ for (c). This fact clearly indicates that if f does not change on the grounds that our gel samples have the same amount of ionizable AAc monomer units, the peak shift to a smaller q results from decreasing ϕ or χ or increasing c_s. However, in our experiment, ϕ is constant ($\phi = \phi_0 = 0.1$) and c_s is zero. Just a simple decrease in χ leads to disappearance of the peak itself. Therefore, the fitting result in Figure 4b definitely indicates a decrease in f from 0.0457 to 0.0184 despite the same AAc ratio. This may be due to the "ion condensation effect", as discussed later.

Figure 7 shows a diagram of the ionic atmosphere in (a) redox-mono-AAc and (b) UV-poly-AAc gels. The ellipses with minus sign and circles with plus sign describe AAc monomer units and counterions, respectively. The toned circles around the ellipses, solid curves, and closed circles are the Debye screening radius, NIPAm polymer chains, and cross-linking points, respectively. In Figure 7a, 32 mM AAc monomer units are randomly distributed and are fully ionized. Therefore, the degree of ionization, f, is accurately calculated to be 0.0457 (=32/700), as supported by SANS analysis. In addition, the Debye screening length, k^{-1}, is estimated by the following equation:[3]

$$\kappa^2 = \frac{4\pi l_B}{a^3}\sum_i (z_i\phi_{s,i} + \alpha\phi) \tag{18}$$

where l_B, a, $\phi_{s,i}$, a, and ϕ are the Bjerrum length, the NIPAm monomer length, the fraction of salt of kind i having the valency z_i, the degree of ionization, and the polymer volume fraction,

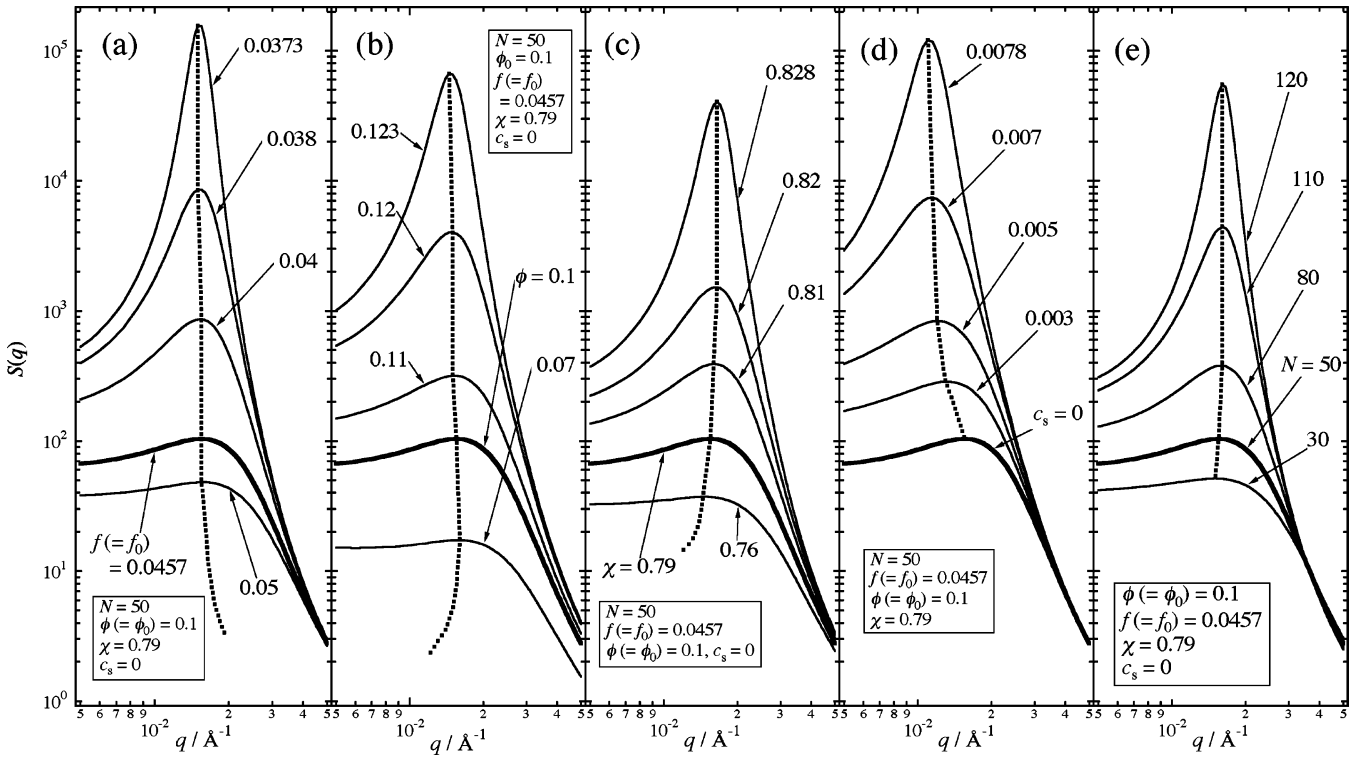

Figure 6. Simulated structure factor, $S(q)$, with RP theory: Each graph shows dependence on (a) f, (b) ϕ, (c) χ, (d) c_s, and (e) N. Thick dotted line in each graph from (a) to (e) shows the trajectory of peak position during the parameters change.

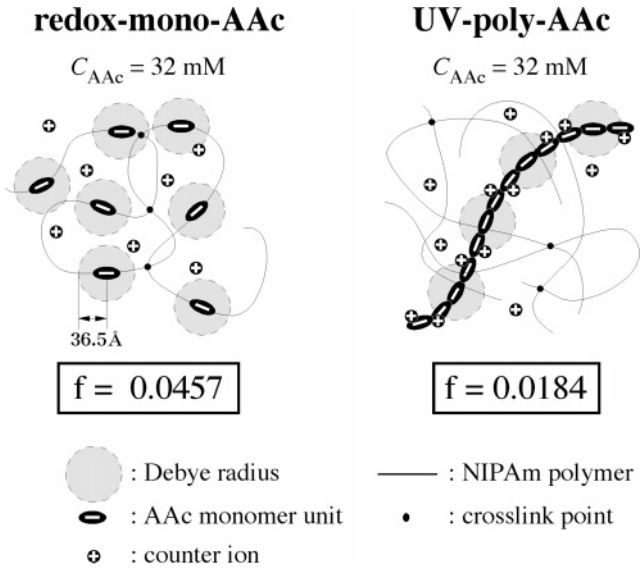

Figure 7. Diagram of the ionic atmosphere in (a) redox-mono-AAc and (b) UV-poly-AAc gels: The ellipses with minus sign and circles with plus sign describe AAc monomer units and counterions, respectively. The toned circles around the ellipses, solid curves, and closed circles are the Debye radius, NIPAm polymer, and cross-linking points, respectively.

respectively. In this case, k^{-1} is estimated to be 36.5 Å, as shown in Figure 7. On the other hand, in the case of UV-poly-AAc gel, the AAc monomer units are tied together side by side to form a polymer chain, as shown in Figure 7b. Here, the electrostatic attraction of counterions to polymer dominates over the entropic gain due to dispersion of the counterions. Therefore, the counterions remain within a short distance of the polymer, leading to neutralization of ionized AAc units.[50−55] As a result, the effective degree of ionization of the UV-poly-AAc gel is much smaller than that of the redox-mono-AAc gel, resulting in a smaller swelling and a lower T_{VPT}, as shown in Figure 2.

The slope of $I(q)$ at $T > T_{VPT}$ in Figure 4c is ca. −4, indicating a macroscopic phase separation. Though charged AAc polymers are present in the gel network, this phenomenon was the same as that observed for NIPAm homopolymer gels. Indeed, T_{VPT} of redox-poly-AAc gel was the same as that of NIPAm homopolymer gel, as shown in Figure 2. This indicates that charged polymers unbound to a gel network do not affect the swelling properties of the gel.

The fact that UV-poly-AAc gel shows strong counterion condensation in a gel network suggests the feasibility of controlling gel microstructure. So far, once weakly charged gel is polymerized with a certain composition, the gel microstructure has been described on the basis of parameters (T, c_s, solvent, f, ϕ, etc.) averaged over the whole gel. But, the results disclosed in this study indicate that the gel microstructure can be tuned by playing with the configuration of ionizable monomer units, even if the whole network composition is set to be the same.

Conclusion

Swelling and SANS measurements were carried out on partially ionized temperature-sensitive polymer gels, poly(NIPAm-AAc). It was found that different gel microstructures can be formed by designing different spatial configurations of ionizable groups in polymer gels. UV-induced NIPAm/poly-AAc (UV-poly-AAc) copolymer gel having localized arrangement of charged groups undergoes microphase separation with a longer period than that of NIPAm-AAc copolymer gel produced by redox method (redox-mono-AAc). The latter has a random distribution of charged groups in monomer unit order, resulting in a higher effective degree of ionization than UV-poly-AAc gel due to the ion condensation along the poly-AAc chains. The counterion condensation also results in lowering the gel volume transition temperature of the UV-poly-AAc gel. Indeed, the theoretical analyses with the RP theory disclosed the following: redox-mono-AAc gel does not form the microstructure with the long period similar to UV-poly-AAc gel at T

> T_{VPT},, unless the degree of ionization is lowered from 0.0457 to 0.0184. On the other hand, in redox-poly-AAc gel, poly-AAc is not bound to but physically entrapped into a gel network. Therefore, its presence does not affect the gel structure at the macroscopic and microscopic levels. That is, the redox-poly-AAc gel has almost the same swelling behavior and microstructure as the NIPAm homopolymer gel. These findings demonstrate that the charge configuration in a weakly charged polymer gel can be tuned, and it plays a significant role in the swelling properties and in microscopic structures. In particular, a significant counterion condensation effect is observed when fully charged polymer chains are copolymerized with noncharged monomer. This may open ways to develop new types of gels having novel properties related to the localized charges in a network, such as gels having rapid shrinking capability and high transparency.

References and Notes

(1) Shibayama, M.; Tanaka, T.; Han, C. C. *J. Chem. Phys.* **1992**, *97*, 6842.
(2) Nasimova, I. R.; Karino, T.; Okabe, S.; Nagao, M.; Shibayama, M. *J. Chem. Phys.* **2004**, *121*, 9708.
(3) Shibayama, M.; Ikkai, F.; Inamoto, S.; Nomura, S.; Han, C. C. *J. Chem. Phys.* **1996**, *105*, 4358.
(4) Shibayama, M.; Kawakubo, K.; Ikkai, F.; Imai, M. *Macromolecules* **1998**, *31*, 2586.
(5) Micali, N.; Vasi, C.; Mallamace, F.; Bansil, R.; Pajevic, S.; Sciortino, F. *Phys. Rev. E* **1993**, *48*, 4501.
(6) Hourded, D.; F'alloret, F.; Durand, A.; Lafuma, F.; Audebert, R.; Cotton, J.-P. *Macromolecules* **1998**, *31*, 5323.
(7) Braun, O.; Boue, F.; Candau, F. *Eur. Phys. J.* **2002**, *E7*, 141.
(8) Tanaka, T. *Polymer* **1979**, *20*, 1404.
(9) Shibayama, M.; Tanaka, T. *Adv. Polym. Sci.* **1993**, *109*, 1.
(10) Tanaka, T.; Sato, E.; Hirokawa, Y.; Hirotsu, S.; Peetermans, J. *Phys. Rev. Lett.* **1985**, *55*, 2455.
(11) Annaka, M.; Tanaka, T. *Phase Transitions* **1994**, *47*, 143.
(12) Hirokawa, Y.; Tanaka, T. *J. Chem. Phys.* **1984**, *81*, 6379.
(13) Hirose, Y.; Amiya, T.; Hirokawa, Y.; Tanaka, T. *Macromolecules* **1987**, *20*, 1342.
(14) Hirotsu, S.; Hirokawa, Y.; Tanaka, T. *J. Chem. Phys.* **1987**, *87*, 1392.
(15) Hirose, H.; Shibayama, M. *Macromolecules* **1998**, *31*, 5336.
(16) Kato, E. *J. Chem. Phys.* **2000**, *113*, 1310.
(17) Zhong, X.; Wang, Y.-X.; Wang, S.-C. *Chem. Eng. Sci.* **1996**, *51*, 3235.
(18) Kokufuta, E.; Wang, B.; Yoshida, R.; Khokhlov, A.; Hirai, M. *Macromolecules* **1998**, *31*, 6878.
(19) Schosseler, F.; Ilmain, F.; Candau, S. J. *Macromolecules* **1991**, *24*, 225.
(20) Ikkai, F.; Shibayama, M. *J. Polym. Sci., Part B: Polym. Phys. Ed.* **2005**, *43*, 617.
(21) Schosseler, F.; Skouri, R.; Munch, J. P.; Candau, S. J. *J. Phys. II* **1994**, *4*, 1221.
(22) Moussaid, A.; Candau, S. J.; Joosten, J. G. H. *Macromolecules* **1994**, *27*, 2102.
(23) Onuki, A. *Adv. Polym. Sci.* **1993**, *109*, 63.
(24) Panyukov, S.; Rabin, Y. *Macromolecules* **1996**, *29*, 8530.
(25) Sasaki, S.; Maeda, H. *Phys. Rev. E* **1996**, *54*, 2761.
(26) Rabin, Y.; Panyukov, S. *Macromolecules* **1997**, *30*, 301.
(27) Shiwa, Y. *Eur. Phys. J. B* **1998**, *1*, 345.
(28) Tanaka, T.; Annaka, M. *J. Intell. Mater. Syst. Struct.* **1993**, *4*, 548.
(29) Annaka, M.; Tanaka, T. *Nature (London)* **1992**, *355*, 430.
(30) Tanaka, T.; Sun, S. T.; Hirokawa, Y.; Katayama, S.; Kucera, J.; Hirose, Y.; Amiya, T. *Nature (London)* **1987**, *325*, 796.
(31) Ikkai, F.; Adachi, E. *Macromol. Rapid Commun.* **2004**, *25*, 1514.
(32) Shibayama, M.; Shirotani, Y.; Hirose, H.; Nomura, S. *Macromolecules* **1997**, *30*, 7307.
(33) Shibayama, M. Multiphases in Polymeric Gels. In *Structure and Properties of Multi-Phase Polymeric Materials*; Araki, T., Tran-Cong, Q., Shibayama, M., Eds.; Marcel Dekker: New York, 1998; Chapter 6, p 195.
(34) Hirotsu, S. *J. Chem. Phys.* **1991**, *94*, 3949.
(35) Kubota, K.; Fujishige, S.; Ando, I. *Polym. J.* **1990**, *22*, 15.
(36) Ikkai, F.; Adachi, E. *Macromol. Chem. Phys.*, in press.
(37) Suzuki, T.; Ikkai, F.; Shibayama, M. *Macromolecules*, in press.
(38) Okabe, S.; Nagao, M.; Karino, T.; Watanabe, S.; Adachi, T.; Shimizu, H.; Shibayama, M. *J. Appl. Crystallogr.* **2005**, *38*, 1035.
(39) Shibayama, M.; Nagao, M.; Okabe, S.; Karino, T. *J. Phy. Soc. Jpn.* **2005**, *74*, 2728.
(40) Shibayama, M.; Isono, K.; Okabe, S.; Karino, T.; Nagao, M. *Macromolecules* **2004**, *37*, 2909.
(41) Debye, P.; Bueche, A. M. *J. Appl. Phys.* **1949**, *20*, 518.
(42) Wu, W.; Shibayama, M.; Roy, S.; Kurokawa, H.; Coyen, L. D.; Nomura, S.; Stein, R. S. *Macromolecules* **1990**, *23*, 2245.
(43) Onuki, A. *J. Phys. II* **1992**, *2*, 45.
(44) Horkay, F.; Hecht, A.-M.; Grillo, I.; Basser, P. J.; Geissler, E. *J. Chem. Phys.* **2002**, *117*, 9103.
(45) Shibayama, M.; Tanaka, T.; Han, C. C. *J. Chem. Phys.* **1992**, *97*, 6829.
(46) Hecht, A. M.; Duplessix, R.; Geissler, E. *Macromolecules* **1985**, *18*, 2167.
(47) Mallam, S.; Horkay, F.; Hecht, A. M.; Geissler, E. *Macromolecules* **1989**, *22*, 3356.
(48) Horkay, F.; Hecht, A. M.; Mallam, S.; Geissler, E.; Rennie, A. R. *Macromolecules* **1991**, *24*, 2896.
(49) Ikkai, F.; Shibayama, M.; Han, C. C. *Macromolecules* **1998**, *31*, 3275.
(50) Manning, G. S. *J. Chem. Phys.* **1969**, *51*, 924.
(51) Manning, G. S. *J. Chem. Phys.* **1969**, *51*, 934.
(52) Stevens, M. J.; Kremer, K. *J. Phys. II* **1996**, *6*, 1607.
(53) Gonzalez-Mozuelos, P.; Olvera de la Cruz, M. *J. Chem. Phys.* **1995**, *103*, 3145.
(54) Nyquist, R. M.; Ha, B.-Y.; Liu, A. J. *Macromolecules* **1999**, *32*, 3481.
(55) Khokhlov, A. R. *J. Phys. A: Math. Gen.* **1980**, *13*, 979.

MA062216C